AIP | Journal of Applied Physics

# High temperature annealing of n-type 4H-SiC: Impact on intrinsic defects and carrier lifetime

Bernd Zippelius, Jun Suda, and Tsunenobu Kimoto

Citation: J. Appl. Phys. **111**, 033515 (2012); doi: 10.1063/1.3681806
View online: http://dx.doi.org/10.1063/1.3681806
View Table of Contents: http://jap.aip.org/resource/1/JAPIAU/v111/i3
Published by the American Institute of Physics.

# High temperature annealing of n-type 4H-SiC: Impact on intrinsic defects and carrier lifetime

Bernd Zippelius,[a] Jun Suda,[b] and Tsunenobu Kimoto[c]
*Department of Electronic Science and Engineering, Kyoto University, Katsura, Nishikyo, Kyoto 615-8510, Japan*

(Received 20 November 2011; accepted 12 January 2012; published online 8 February 2012)

In this paper, the impact of high-temperature annealing of 4H silicon carbide (SiC) on the formation of intrinsic defects, such as $Z_{1/2}$ and $EH_{6/7}$, and on carrier lifetimes was studied. Four nitrogen-doped epitaxial layers with various initial concentrations of the $Z_{1/2}$- and $EH_{6/7}$-centers ($10^{11} - 10^{14}$ cm$^{-3}$) were investigated by means of deep level transient spectroscopy and microwave photoconductance decay. It turned out that the high-temperature annealing leads to a monotone increase of the $Z_{1/2}$- and $EH_{6/7}$-concentration starting at temperatures between 1600 °C and 1750 °C, depending on the initial defect concentration. In the case of samples with high initial defect concentration ($10^{14}$ cm$^{-3}$) a distinct decrease in $Z_{1/2}$- and $EH_{6/7}$-concentration in the temperature range from 1600 °C to 1750 °C was observed, being consistent with previous reports. For higher annealing temperatures ($T_{anneal} \geq 1750$ °C), the defect concentration is independent of the samples' initial values. As a consequence, beside the growth conditions, such as C/Si ratio, the thermal post-growth processing has a severe impact on carrier lifetimes, which are strongly reduced for samples annealed at high temperatures. © *2012 American Institute of Physics*. [doi:10.1063/1.3681806]

## I. INTRODUCTION

During recent years, huge effort has been put into controlling the concentration of intrinsic defects in silicon carbide. In the widely used 4H-SiC, the most prominent representatives $Z_{1/2}$ (Ref. 1) and $EH_{6/7}$ (Ref. 2) are located in the upper half of the bandgap and have a significant impact on the carrier lifetime in SiC,[3,4] which is a physical key property determining the performance of bipolar devices. Many hints have been given in the literature on involvement of the carbon vacancy ($V_C$) in these defects (e.g., Ref. 5). Therefore, the concentration of $Z_{1/2}$ and $EH_{6/7}$ can be lowered, e.g., by C-implantation[6] or oxidation,[7] and the resulting carrier lifetime is greatly improved. Recently, the acceptor states and donor states of $V_C$ have been proposed as the origin of $Z_{1/2}$ and $EH_{6/7}$, respectively;[8] however, this still has to be proven experimentally.

Due to the low diffusion constant of common dopants in SiC, ion implantation is frequently used during device fabrication, e.g., to form p-/n-type regions or contact regions. For removal of implantation damage and for electrical activation of the implanted dopants, high-temperature annealing steps are required. Therefore, knowing the impact of thermal treatment on the concentration of intrinsic defects in SiC is of great importance and may give further insight to the formation mechanisms.

## II. EXPERIMENTAL

Four sets of n-type 4H-SiC epitaxial layers with a by-four-orders-of-magnitude varying initial $Z_{1/2}$-concentration have been investigated (see Table I):

- Sample set (1), for which a commercial n-type 4H-SiC(0001) epitaxial layer (same as set (2)) with a thickness of $d_{epi} \approx 50\mu$m had been irradiated with electrons of an energy of $E(e^-) = 200$keV and a dose of $D(e^-) = 2 \times 10^{16}$ cm$^{-2}$, damaging mainly the carbon sublattice.[9] A preannealing step in a rapid thermal-annealing setup under Ar atmosphere at 950 °C for 30 min was used to remove the carbon interstitial-related defects;[10] the resulting initial $Z_{1/2}$-concentration was $[Z_{1/2}]_{ini} \approx 1.6 \times 10^{14}$ cm$^{-3}$.
- Sample set (2), a commercial n-type epitaxial layer ($d_{epi} \approx 50\mu$m, same material as used for set (1)) containing a net doping concentration of $[N] \approx 1.2 \times 10^{15}$ cm$^{-3}$ and an initial concentration of $[Z_{1/2}]_{ini} \approx 1.5 \times 10^{13}$ cm$^{-3}$ (as-grown).
- Sample set (3), a custom-made (Kyoto University) 4H-SiC(0001) n-type epitaxial layer ($d_{epi} \approx 125\mu$m) with a very low net nitrogen doping concentration of $[N] \approx$ (7 to 9) $\times 10^{13}$ cm$^{-3}$ and a low initial $Z_{1/2}$-concentration of $[Z_{1/2}]_{ini} \approx 1.4 \times 10^{12}$ cm$^{-3}$ (as-grown).
- Sample set (4), for which the epilayer of set (2) had been oxidized for 5 h at 1300 °C prior to the annealing experiments. Directly after oxidation, the oxide was removed by hydrofluoric acid; the initial $Z_{1/2}$-concentration dropped below the detection limit of $2.5 \times 10^{11}$ cm$^{-3}$.

The samples were covered with a carbon cap to prevent surface roughening[11] and isochronally annealed (15 min) in a horizontal hot-wall chemical vapor deposition system at temperatures ranging from 1300 °C to 1850 °C under Ar atmosphere; the carbon cap was subsequently removed by thermal oxidation for 1 h at 800 °C. Schottky contacts with a thickness of 150 nm were prepared by thermal evaporation of nickel through a shadow mask. The backside ohmic contact was realized by silver paste on the highly doped substrate.

[a]Electronic mail: bernd@semicon.kuee.kyoto-u.ac.jp.
[b]Electronic mail: suda@kuee.kyoto-u.ac.jp.
[c]Electronic mail: kimoto@kuee.kyoto-u.ac.jp.

 

TABLE I. Overview of the investigated sample sets with an epilayer thickness $d_{epi}$, a net nitrogen doping $[N]_{net}$, and an initial $Z_{1/2}$-concentration $[Z_{1/2}]_{ini}$.

| Sample set | $d_{epi}(\mu m)$ | $[N]_{net}(cm^{-3})$ | $[Z_{1/2}]_{ini}(cm^{-3})$ | Remarks |
|---|---|---|---|---|
| (1) | 50 | $\approx 1.2 \times 10^{15}$ | $\approx 1.6 \times 10^{14}$ | electron irradiation. of set (2): $E(e^-) = 200\,keV$, $D(e^-) = 2 \times 10^{16}\,cm^{-2}$. Annealing: 950 °C/30 min |
| (2) | 50 | $\approx 1.2 \times 10^{15}$ | $\approx 1.5 \times 10^{13}$ | Commercial |
| (3) | 125 | $\approx (7\,to\,9) \times 10^{13}$ | $\approx 1.4 \times 10^{12}$ | Custom-made (Kyoto-Univ.) |
| (4) | 50 | $\approx 1.2 \times 10^{15}$ | $< 2 \times 10^{11}$ | Oxidation of set (2): 1300 °C/5 h |

The defect concentration was monitored by means of deep level transient spectroscopy (DLTS) in a temperature range between 200 K and 720 K. The measurements were taken with reverse bias of $V_R = -10$ V, pulse bias of $V_P = -0.5$ V, filling pulse time of $t_P = 1$ ms, and time window of $T_W = 204.8$ ms.

Furthermore, measurements of the carrier lifetime by the differential microwave photoconductance decay ($\mu$-PCD) method have been conducted. A pulsed yttrium lithium fluoride 3rd harmonic generation (YLF-3HG) laser with a wavelength of 349 nm was used to generate excess carriers. The applied photon density corresponds to a generated density of electron-hole pairs of $3.6 \times 10^{16}$ cm$^{-3}$ at the surface. The conductance decay was monitored by the reflectivity of microwaves with a frequency of 26 GHz. To increase the signal-to-noise ratio, the difference of reflectivity between areas without and with illumination was used as $\mu$-PCD signal.

## III. RESULTS AND DISCUSSION

### A. Deep level transient spectroscopy

Figure 1(a) shows the normalized DLTS spectra of the non-annealed reference samples, sets (1) – (4). The peak height corresponds to the defect concentration as the DLTS spectra are normalized to the doping concentration. The irradiated (dotted line) and as-grown samples (solid and dashed lines) show the dominating defects $Z_{1/2}$ ($E_C - 0.67$eV) and $EH_{6/7}$ ($E_C - 1.55$eV), whereas, in the oxidized sample (dash-dotted line), their concentration lies below the detection limit. The DLTS spectra of the samples which have been annealed at 1850 °C for 15 min are depicted in Fig. 1(b): The $Z_{1/2}$- and $EH_{6/7}$-signals are nearly identical and independent of the initial concentration.

The concentrations of the ON1- ($E_C - 0.9$eV) and ON2a/b-defect ($E_C - 1.0$eV), which usually emerge in oxidized or C-implanted samples,[12] are nearly independent of the annealing temperature. It is assumed that the carbon interstitial ($I_C$) is involved in these defects. To conduct depth profiling within the first 8 $\mu$m from the surface, the reverse voltage during DLTS measurements was varied up to $V_R = -100$V and a decrease of ON1- and ON2a/b-concentration by a factor of approximately 5 could be observed (not shown). In contrast, the obtained depth profile of the $Z_{1/2}$-concentration is constant in this near-surface region for all samples.

Figure 2 shows the observed concentration of (a) $Z_{1/2}$- and (b) $EH_{6/7}$-centers as a function of the annealing temperature $T_{anneal}$ for all samples. The initial $Z_{1/2}$-concentration lies in the range from $2.5 \times 10^{11}$ cm$^{-3}$ to $1.4 \times 10^{14}$ cm$^{-3}$ (very left symbols); the $EH_{6/7}$-concentration is slightly lower ($2.5 \times 10^{11}$ cm$^{-3}$ to $1.0 \times 10^{14}$ cm$^{-3}$). In the case of set (4) (open circles), the values are an upper limit of the defect concentrations, as they are below the detection limit. For the irradiated samples (set (1), triangles), a first decline in $Z_{1/2}$- and $EH_{6/7}$-concentration can be observed at temperatures between 950 °C (after preannealing step) and 1400 °C,

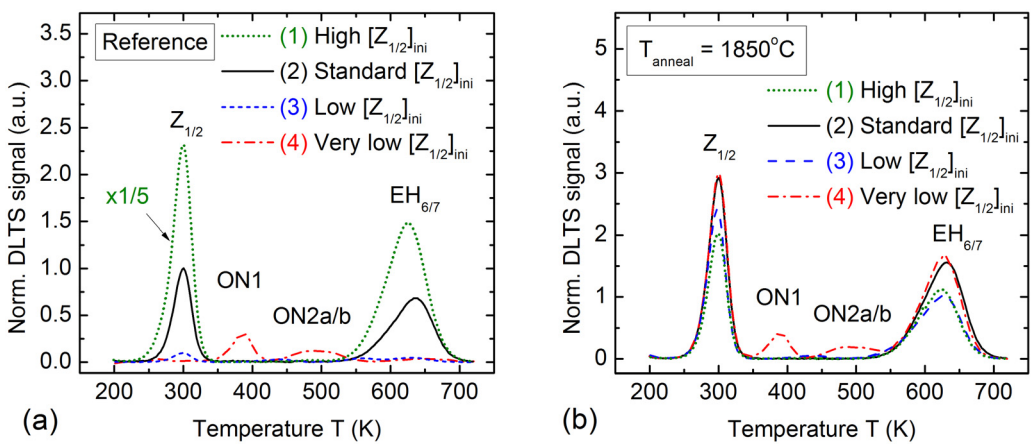


FIG. 1. (Color online) Normalized DLTS spectra taken on samples with (1) high (electron irradiated, dotted line), (2) standard (as-grown (commercial), solid line), (3) low (as-grown (Kyoto-University), dashed line), and (4) very low (oxidized, dash-dotted line) initial $Z_{1/2}$-concentration, which (a) have not been annealed and (b) have been annealed at 1850 °C for 15 min. The annealed samples show nearly identical $Z_{1/2}$-signals, which are even higher than that of sample (1) (Fig. 1(a)). The spectra depict the sine-correlation $b_1$ normalized by net doping and capacitance under reverse bias at room temperature ($b_{1,norm} = b_1 N_{net}/C_R$) with a time window of $T_W = 204.8$ms. The measurements were taken with reverse bias of $V_R = -10$V, pulse bias of $V_P = -0.5$V, and filling pulse time of $t_P = 1$ms.

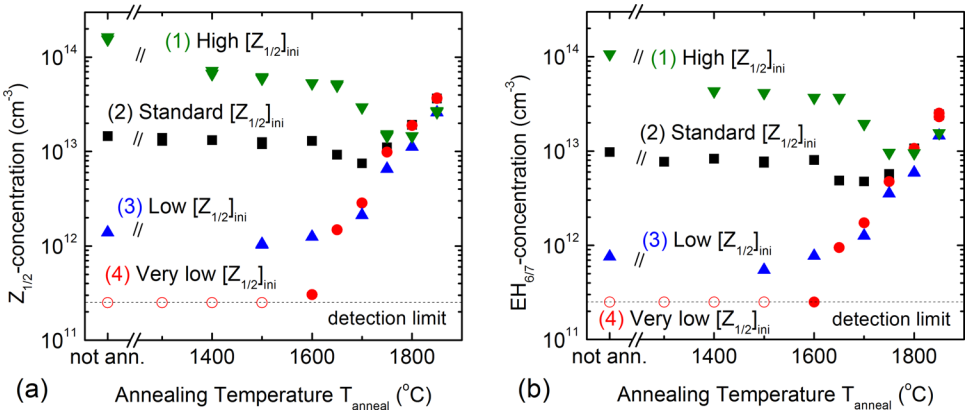


FIG. 2. (Color online) (a) $Z_{1/2}$- and (b) $EH_{6/7}$-concentration of set (1) to (4) vs annealing temperature. The very left measurement points show the by-orders-of-magnitude varying initial concentration of the reference samples, which have not been annealed. In the case of the oxidized samples, the concentrations are an upper limit, as they lie below the detection limit (open circles).

resulting in a concentration of $[Z_{1/2}] = (5 \text{ to } 7) \times 10^{13}$ cm$^{-3}$ and $[EH_{6/7}] = (3 \text{ to } 5) \times 10^{13}$ cm$^{-3}$, respectively. In the temperature range of 1600 °C and 1750 °C, a second, stronger decrease of both defect concentrations is detected, consistent with the findings of previous publications.[10,13–15] When reaching even higher temperatures, the defect concentrations are increasing again. The samples of set (2) (squares) show a similar behavior, with nearly constant concentrations of $[Z_{1/2}] = (1.0 \text{ to } 1.5) \times 10^{13}$ cm$^{-3}$ and $[EH_{6/7}] = (8 \text{ to } 10) \times 10^{12}$ cm$^{-3}$, respectively, up to annealing temperatures of 1600 °C and a weak decrease until 1700 °C. For higher temperatures, they show the same trend and almost identical concentrations as set (1). Defect concentration of set (3) (triangles) stays constant up to a temperature range between 1600 °C and 1700 °C and then follows the increase of the other samples. In the case of the oxidized samples (set (4), circles), a distinct increase of $Z_{1/2}$- and $EH_{6/7}$-concentrations can be already observed from 1600 °C. In summary, depending on the initial defect concentration, the other samples (sets (1)–(3)) follow this specific increase after annealing above a certain temperature, and the resulting $Z_{1/2}$- and $EH_{6/7}$-concentrations are nearly identical, independent of the initial trap concentrations. Therefore, temperature seems to be a driving force for the generation of carbon vacancies, beside the growth conditions, such as the C/Si ratio. As the defect concentrations are closely lying together, the system may be near thermal equilibrium.

On the one hand, the driving force for the formation of intrinsic defects, such as interstitials and vacancies, is the irreversibly increasing entropy $S$: with every deviation from a perfect crystal, the system's entropy is enlarged. On the other hand, a defined formation energy (also effective enthalpy) $E_f$ is required to create defects, resulting in the free energy of formation,

$$F_f = E_f - TS. \quad (1)$$

The concentration of a simple defect under thermal equilibrium then is determined by[16]

$$N_T = N_0 \exp\left(-\frac{F_f}{k_B T}\right), \quad (2)$$

with $N_0$ as the concentration of lattice sites where the defect may reside, $k_B$ as the Boltzmann constant, and $S$ as the formation entropy of the defect. With the concentration of carbon lattice sites in SiC of $4.8 \times 10^{22}$ cm$^{-3}$, the theoretical values for $E_f$ and $S$ of the carbon vacancy, it seems possible to predict an equilibrium concentration of $Z_{1/2}$ (under the assumption that it consists only of a single $V_C$). However, as there are relatively big uncertainties in $E_f$, an exact value for the trap concentration cannot be given. Additionally, since the calculation of the entropy requires very high computational power, it is usually neglected, which can be justified for moderate temperatures.[17] In the case of Si or GaAs, the calculated entropy for vacancies ranges from 5 $k_B$ to 10 $k_B$.[16,18] From Eqs. (1) and (2), the defect concentration under thermal equilibrium can be obtained from[19]

$$N_T = N_0 \exp\left(\frac{S}{k_B}\right)\exp\left(-\frac{E_f}{k_B T}\right) = A\exp\left(-\frac{E_f}{k_B T}\right). \quad (3)$$

As the $Z_{1/2}$- and $EH_{6/7}$-concentrations for $T_{anneal} > 1700$ °C are almost the same for all samples, independent of the initial defect concentration, the system is close to thermal equilibrium and Eq. (3) may be valid. Due to a quite fast cooling-down (from 1850 °C to 1600 °C within 1 min), the system is "conserved" in its high temperature state. By an Arrhenius plot of the trap concentration of $Z_{1/2}$ and $EH_{6/7}$ versus the inverse annealing temperature, their formation energy can be obtained from the slope (see Fig. 3). The Arrhenius analysis was conducted only for samples of set (3) and (4), since, here, an exponential increase can be observed for more than three data points. The values for the formation energy are approximately 6.4 eV to 6.6 eV for the $Z_{1/2}$-center (see Fig. 3(a)) and 5.7 eV to 6.1 eV for the $EH_{6/7}$-center (see Fig. 3(b)).

These values are slightly larger than the formation energy of 4.6±0.3 eV for both $Z_{1/2}$ and $EH_{6/7}$, obtained from experiments by varying the growth temperature.[19] The theoretical formation energy of the carbon vacancy under stoichiometric conditions varies from 4.2 eV (4H-SiC)[20] to 5.9 eV (3C-SiC),[21] which is slightly lower than the correspondingly detected formation energy for $Z_{1/2}$ and $EH_{6/7}$ during the annealing experiments.

This difference could possibly be attributed to slightly different formation mechanisms during growth and annealing, respectively. Possible formation mechanisms of the carbon vacancy during annealing are (i) the creation of Frenkel

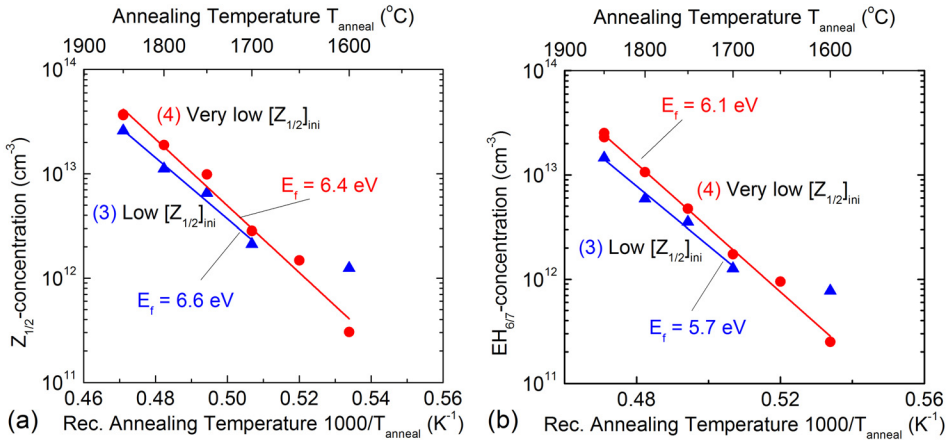


FIG. 3. (Color online) (a) $Z_{1/2}$- and (b) $EH_{6/7}$-concentration vs reciprocal annealing temperature. From the slope of the Arrhenius plot for the sample sets (3) and (4), the formation energy is determined after Eq. (3) as (a) $E_f(Z_{1/2}) = 6.4 - 6.6$eV and (b) $E_f(EH_{6/7}) = 5.7 - 6.1$eV.

pairs ($V_C - I_C$ pairs) in the epilayer, (ii) the formation of Schottky defects ($V_C - V_{Si}$ pairs) near the surface with subsequent diffusion of carbon vacancies into the bulk, and, further, (iii) the formation of $V_C$ by diffusion from the substrate, where a high concentration of vacancies is present. It is not clear at present which process is responsible for the increase of $Z_{1/2}$- and $EH_{6/7}$-centers during the annealing; the authors speculate that $V_C$ diffusion from the substrate cannot be neglected.

The substrate might serve as a possible source of vacancies and, therefore, a diffusion process will mainly determine the formation energy of the $Z_{1/2}$- and $EH_{6/7}$-center in this case. During the annealing process in this study, the Fermi level reaches a midgap position and the charge state of the carbon vacancy will be in the transition region from $V_C^0$ (n-type material) to $V_C^{2+}$ (intrinsic/p-type material). Bockstedte *et al.*[16] calculated the migration barriers as 3.5 eV and 5.2 eV for the neutral and the doubly positively charged carbon vacancy in 3C-SiC, respectively. Theoretical diffusivity calculations by Rauls *et al.*[17] for 4H-SiC, including vibrational entropy correction, result in similar values (4.4 eV for $V_C^0$ and 5.5 eV for $V_C^{2+}$ at 1800 K). However, they state that the obtained diffusion length of less than 1 $\mu$m at 1800 K is probably too small, as an out-diffusion of $V_C$ was experimentally observed already at lower temperatures ($T_{anneal} = 1600\,^{\circ}C$).[22] In the present study, this temperature is around the starting point for the increase of defect concentration in the oxidized samples as well as the starting point for the defect reduction in the case of the irradiated samples (Fig. 2). This defect reduction is probably due to out-diffusion of C-vacancies toward the surface, since after the 950 °C preannealing step, no other defects beside the $Z_{1/2}$- and $EH_{6/7}$-centers are observed in the upper bandgap. Therefore, a recombination process with C-interstitial related defects seems negligible. To identify the exact process of carbon vacancy generation at high temperature, further investigations are required.

## B. Lifetime measurement

For monitoring lifetime $\tau$ in the various epilayers, $\mu$-PCD measurements have been conducted in mapping mode (Fig. 4). For this, decay curves have been sampled in steps of 1 mm in each direction and $\tau$ has been calculated from the slope of the decay curve at the point where it reaches $1/e^2$ of its initial value. Lifetime is rather homogeneous over the area for the particular samples. $\tau$ is correlated to the initial $Z_{1/2}$-concentration and varies from 0.12 $\mu$s to 1.9 $\mu$s (see first row of Fig. 4 and very left symbols in Fig. 5). However, in the case of the oxidized sample (set (4), circles), with an initial $Z_{1/2}$-concentration below the detection limit, $\tau$ is smaller compared to the sample of set (3) (triangles) with $[Z_{1/2}]_{ini} \approx 1.4 \times 10^{12}$ cm$^{-3}$. This difference is most likely due to recombination via HK0-center emerging after oxidation.[23] This is supported by the observed increase in lifetime for samples of set (4), which have been annealed at 1400 °C to 1600 °C, when HK0 is strongly reduced.[23] Another reason for this difference in lifetime could be a stronger influence of the substrate recombination,[24] since the thickness of the epitaxial layer of set (4) is about a factor of 2 thinner than that of set (3). In oxidized samples (set (4)) annealed at 1400 °C, the overall largest value of 2.4 $\mu$s was measured at room temperature. After annealing at 1850 °C, the lifetime lies between 0.25 $\mu$s and 0.5 $\mu$s for all samples (Fig. 5). In the case of the irradiated samples, an improvement of the carrier lifetime could be observed, as the $Z_{1/2}$-concentration is lower compared to the initial status. For all other samples, lifetime is reduced by thermal treatment over 1600 °C. The inverse carrier lifetime

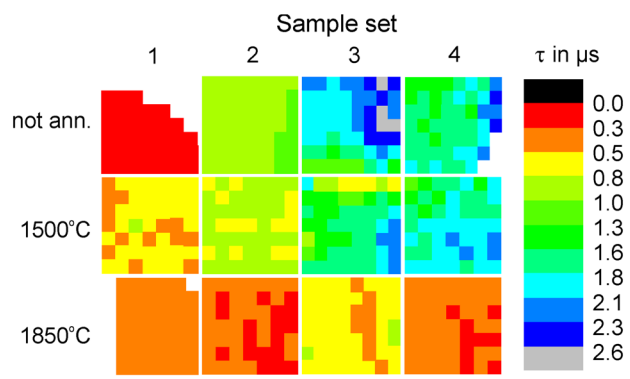


FIG. 4. (Color online) Mapping of the $\mu$-PCD lifetime for non-annealed samples (first row) and samples which have been annealed at 1500 °C (second row) and at 1850 °C (third row), respectively, of each sample set. $\tau$ is relatively uniformly distributed inside each sample and depends on the respective $Z_{1/2}$-concentration.

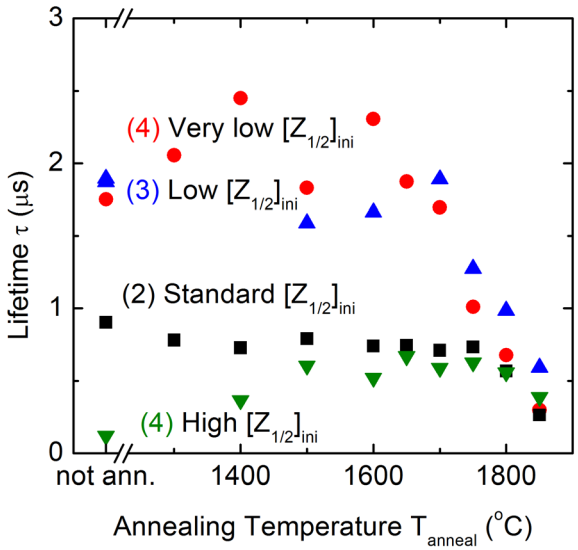


FIG. 5. (Color online) Lifetime obtained by $\mu$-PCD as a function of the annealing temperature. The lifetime is decreasing as the concentration of $Z_{1/2}$ is reaching values larger than $10^{13}$ cm$^{-3}$.

is strongly correlated to the concentration of the $Z_{1/2}$-center above a value of $10^{13}$ cm$^{-3}$, which is consistent with previous reports,[25] verifying it as the lifetime killer.

## IV. CONCLUSION

It has been shown that high-temperature annealing, as it is used for electrical activation of implanted dopants during device fabrication, has a great impact on the formation of the $Z_{1/2}$- and $EH_{6/7}$-centers in 4H-SiC. For samples with a very low initial concentration of $Z_{1/2}$ and $EH_{6/7}$, an increase of the defect concentration can be observed for temperatures $T_{\text{anneal}} > 1600\,^{\circ}$C. The decrease in $Z_{1/2}$- and $EH_{6/7}$-concentration in the temperature range from 1600 °C to 1750 °C in the case of samples with high initial defect concentration is in accordance with previous publications and might be attributed to out-diffusion of vacancies toward the surface, as no other defects besides the $Z_{1/2}$- and $EH_{6/7}$-center have been observed. For annealing temperatures $T_{\text{anneal}} \geq 1750\,^{\circ}$C, the detected concentrations of $Z_{1/2}$ and $EH_{6/7}$ do not depend on the initial conditions. Furthermore, a reduction of the carrier lifetime was observed due to the increase in $Z_{1/2}$-concentration, which is in agreement with previous reports. Thus, lifetime-enhancing treatment during device processing, such as oxidation steps, should be conducted after high-temperature treatments. If this is not possible, an annealing temperature below 1750 °C should be chosen with the trade-off of less electrically activated dopants.

## ACKNOWLEDGMENTS

This work was supported by the Funding Program for World-Leading Innovative R&D on Science and Technology (FIRST Program) and Grant-in-Aid for Scientific Research (21226008) from the Japan Society for the Promotion of Science.

[1]T. Dalibor, C. Peppermüller, G. Pensl, S. Sridhara, R. P. Devaty, W. J. Choyke, A. Itoh, T. Kimoto, and H. Matsunami, Inst. Phys. Conf. Ser. **142**, 517 (1996).
[2]C. Hemmingsson, N. T. Son, O. Kordina, J. P. Bergman, E. Janzén, J. L. Lindström, S. Savage, and N. Nordell, J. Appl. Phys. **81**, 6155 (1997).
[3]P. B. Klein, Phys. Status Solidi A **206**, 2257 (2009).
[4]K. Danno, D. Nakamura, and T. Kimoto, Appl. Phys. Lett. **90**, 202109 (2007).
[5]L. Storasta, J. P. Bergman, E. Janzén, A. Henry, and J. Lu, J. Appl. Phys. **96**, 4909 (2004).
[6]L. Storasta and H. Tsuchida, Appl. Phys. Lett. **90**, 062116 (2007).
[7]T. Hiyoshi and T. Kimoto, Appl. Phys. Express **2**, 041101 (2009).
[8]T. Hornos, A. Gali, and B. G. Svensson, Mater. Sci. Forum **679–680**, 261 (2011).
[9]A. A. Rempel, W. Sprengel, K. Blaurock, K. J. Reichle, J. Major, and H.-E. Schaefer, Phys. Rev. Lett. **89**, 185501 (2002).
[10]K. Danno and T. Kimoto, J. Appl. Phys. **100**, 113728 (2006).
[11]Y. Negoro, K. Katsumoto, T. Kimoto, and H. Matsunami, J. Appl. Phys. **96**, 224 (2004).
[12]L. Storasta, H. Tsuchida, T. Miyazawa, and T. Ohshima, J. Appl. Phys. **103**, 013705 (2008).
[13]M. Weidner, T. Frank, G. Pensl, A. Kawasuso, H. Itoh, and R. Krause-Rehberg, Physica B **308–310**, 633 (2001).
[14]Y. Negoro, T. Kimoto, and H. Matsunami, Appl. Phys. Lett. **85**, 1716 (2004).
[15]G. Alfieri, E. V. Monakhov, B. G. Svensson, and M. K. Linnarsson, J. Appl. Phys. **98**, 043518 (2005).
[16]M. Bockstedte, M. Heid, and O. Pankratov, Phys. Rev. B **67**, 193102 (2003).
[17]E. Rauls, T. Frauenheim, A. Gali, and P. Deák, Phys. Rev. B **68**, 155208 (2003).
[18]P. E. Blöchl, E. Smargiassi, R. Car, D. B. Laks, W. Andreoni, and S. T. Pantelides, Phys. Rev. Lett. **70**, 2435 (1993).
[19]K. Danno, T. Hori, and T. Kimoto, J. Appl. Phys. **101**, 53709 (2007).
[20]L. Torpo, M. Marlo, T. E. M. Staab, and R. M. Nieminen, J. Phys.: Condens. Matter **13**, 6203 (2001).
[21]C. Wang, J. Bernholc, and R. F. Davis, Phys. Rev. B **38**, 12752 (1988).
[22]N. T. Son, B. Magnusson, Z. Zolnai, A. Ellison, and E. Janzén, Mater. Sci. Forum **433–436**, 45 (2003).
[23]T. Hiyoshi and T. Kimoto, Appl. Phys. Express **2**, 091101 (2009).
[24]T. Kimoto, T. Hiyoshi, T. Hayashi, and J. Suda, J. Appl. Phys. **108**, 083721 (2010).
[25]T. Kimoto, K. Danno, and J. Suda, Phys. Status Solidi B **245**, 1327 (2008).